1   Application of Electrochemical Impedance Spectroscopy to evaluate

2   cathodically protected coated steel in seawater

3   M. Narozny[1], K. Zakowski[1], K. Darowicki[1]

4   [1] Department of Electrochemistry, Corrosion and Materials Engineering, Chemical Faculty, Gdansk

5   University of Technology, 11/12 Narutowicza St., 80-233, Gdansk, Poland

6   Corresponding author e-mail: michal.narozny@pg.gda.pl

7   Abstract:

8   Two types of organic coated carbon steel (S235JR2 grade) electrodes were exposed to artificial

9   seawater environment. One prepared type was defect free while the other one had an intentionally

10   introduced φ0,5 cm coating defect. Both kinds of samples were polarized during the exposure to four

11   potentials corresponding to four different cathodic protection levels. Evolution of their EIS spectra is

12   presented in this paper. Results obtained in the experiment indicate that protective organic coating

13   condition could be estimated and monitored in time based on EIS investigations. If a sample is defected

14   EIS allows a recognition of overprotected and unprotected sample. Distinguishing a fully protected

15   sample from partially protected sample based on EIS was troublesome.

16   Keywords: Organic coatings; Cathodic Protection; Seawater; Electrochemical Impedance

17   Spectroscopy; Steel.

1. Introduction

19   Organic coatings are the most often and commonly used anti-corrosion technique [1-2]. Coatings

20   provide passive barrier against the aggressive environment. However, coatings provide protection as

21   long as they remain intact and active pigments are not replenished [3-4]. On the other hand, cathodic

22   protection (CP) system is capable of reducing corrosion rate even if a coating fails. CP is an

23   electrochemical technique thus it's not capable of stopping corrosion completely but it significantly

24   reduces its rate [5-6]. Organic coatings and CP are jointly used to provide a holistic anti corrosion

25   protection [7]. Without a coating current demand of CP system could be so great that it might be

26   technically impossible to implement. A proper coating system may reduce current demand by over

27   99 %. Even after years of operation coatings can reduce cathodic current demand by 70-80% or more

28   [8]. However, it is important to remember that certain coatings are not compatible with CP systems.

29   Therefore it remains a factor which has to be taken into account when a complex corrosion protection

30 system is designed [9]. A working CP system produces OH⁻ ions at the cathode increasing the alkalinity

31 of the environment. There is always a risk that an ill-working CP system may cause coating

32 deterioration and disbondment [10-12]. Especially if a critical potential is reached and water

33 decomposition and hydrogen evolution occurs [13-15]. A cathodic protection system can rapidly

34 increase coating deterioration if it has been not been properly supervised.

35 Modern CP rectifiers are often controlled by microcomputers. Unlike old manually adjustable units

36 functionality of the modern rectifiers can be easily extended. CP rectifiers could be equipped with

37 automatic on/off switcher, GPS time stamp, data logger and transmission unit, a watchdog, electric

38 resistance corrosion coupon probe electrode, array of reference electrodes for stray current detection

39 or other devices [16-21]. Due to the rapid electronic device development even Electrochemical

40 Impedance Spectroscopy (EIS) module could be fit [22]. EIS is a technique capable of yielding

41 information about impedance of the investigated system in the investigated frequency bandwidth. EIS

42 data can be linked to the occurring electrochemical processes or physical properties of the investigated

43 system [23-25].

44 In this paper an experiment involving EIS investigation of S235JR2 grade steel samples coated with

45 organic coating under several cathodic protection conditions has been proposed. The coatings have

46 been immersed in seawater for as long as 9 months. EIS data has been collected in order to verify its

47 usefulness as a supplementary CP evaluation technique.
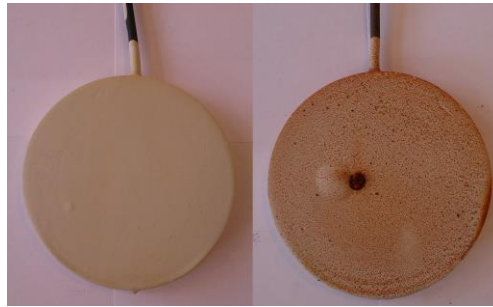
48 2. Materials and methods

49 A set of circular steel electrodes made of S235JR2 was manufactured. Composition of S235JR2 is

50 presented in Tab. 1. Their radius equalled 6 cm and surface area 28,25 cm². Steel substrates and cable

51 connectors were embedded in epoxy resin and insulated from environment.

Element Ultimate Tensile Strength	C [%]	Mn [%]	Si [%]	P [%]	S [%]	N [%]	UTS [N/mm2]
S235JR steel	0,17-0,20	Max 1,3	-	0,045	0,045	0,009	360-490

52 Tab. 1 Composition and ultimate tensile strength of S235JR2 steel.

53 Specimen were sandblasted to the Sa3 NACE "white metal blast cleaning" surface roughness [26].

54 Substrates have been covered with a commercially available epoxy coating. According to the product

55 specification the coating was designed to be applied as a single or multi-layer system. The coating was

56 also confirmed to be CP compatible. Average coating thickness equalled 350 µm and its standard

57 deviation 13 µm. Two sets of samples were prepared. One type of specimen was defect-free, the other

58 one had a Φ0,5 cm holiday (Fig. 1).

59 Furthermore, weight loss coupons made of 100 cm^2 S235JR2 steel grade were manufactured and were

60 exposed under the same conditions as the test specimens. They were prepared accordingly with EIS

61 specimen.

62

63 Fig. 1 Samples after exposure. A defect-free sample (left) and a sample with Φ 0,5 cm holiday (right).

64 In accordance to European Standard EN 12473 "General principles of cathodic protection in sea water"

65 four potentials corresponding to four different cathodic protection levels were chosen (Tab. 2)**Błąd!**

66 **Nie można odnaleźć źródła odwołania.**. For every protection level a separate set of samples (no

67 holiday/ Φ0,5 cm holiday) was prepared. During the entire exposure duration for every cathodic

68 protection level a dedicated potentiostat was assigned to control electrochemical potential of

69 specimen. Specimen were immersed in 50x20x30 cm tanks filled with 30 l of artificial seawater.

70 Artificial sea water composition was prepared in agreement with ASTM D1141-98 standard. Details are

71 presented in Tab. 3 [27]. Salts with content lower than KBr were not used.

Cathodic protection level	Potential vs Zn/ZnSO$_4$ (saturated) [mV]	Potential vs Ag|AgCl|Seawater [mV]
No protection	Free corrosion potential On average +363	Free corrosion potential, On average -675
Under protection	+288 mV	-750
Full protection	+88 mV	-950
Overprotection	-162 mV	-1200

72 Tab. 2 Cathodic protection levels and potentials of specimen.

73 Anodes – auxiliary electrodes made of 20x15 cm mixed metal oxide covered titanium mesh were

74 utilized. Saturated Zn|ZnSO$_4$ reference electrodes were chosen and placed as close as possible to the

75 specimen in order to reduce IR drop. In order to ensure a good cathodic current distribution anodes

76 were located as far away from the working electrodes as possible. During the exposure weigh loss

77 coupons and samples were electrically shortened. For EIS experiments Ag|AgCl|Seawater reference

78 electrode was used. Every sample was then electrically disconnected and evaluated separately.

Salt	NaCl	MgCl$_2$	Na$_2$SO$_4$	CaCl$_2$	KCl	NaHCO$_3$	KBr
Concentration [g/dm^3]	24,53	5,20	4,09	1,16	0,695	0,201	0,101

79 Tab. 3 Artificial seawater composition according to ASTM D1141-98.

80 Every few days Electrochemical Impedance Spectroscopy experiments were performed. In the

81 beginning of the exposure intervals between experiments were short: ranging from 2 to 7 days. Once

82 specimen condition stabilized measurements were taken less often – and intervals increased from 7

83 to 30 days. Perturbation amplitude equalled 15 mV and frequency bandwidth ranged from 0,05 Hz to

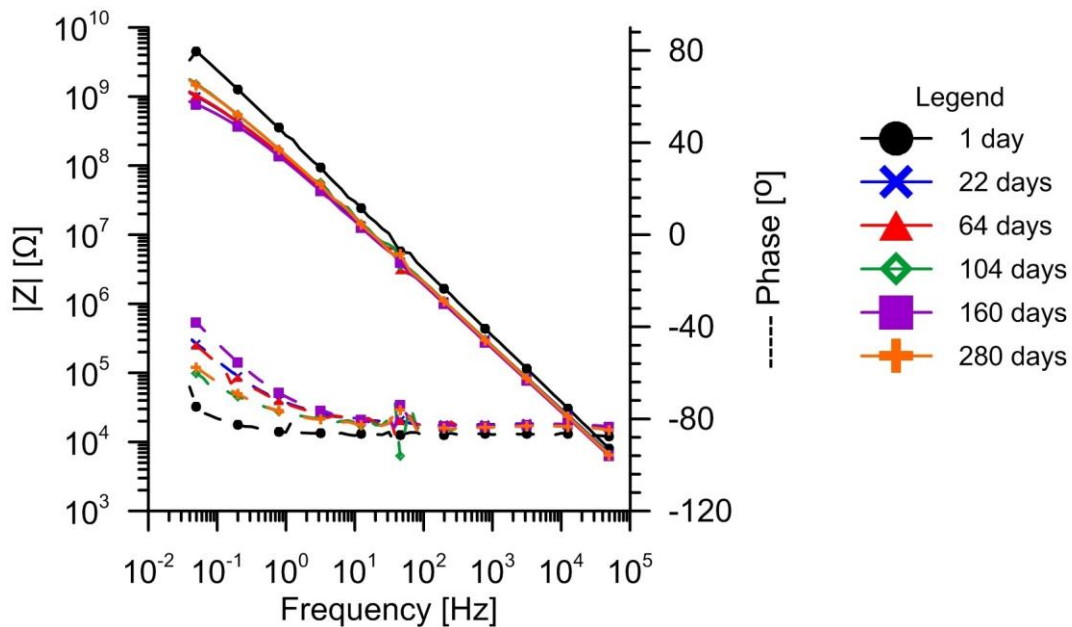84 10 kHz. All tests were carried out using Gamry 1000 potentiostat.

85 3. Results and discussion

86 Long term exposure of coated specimen were performed in order to review applicability of EIS to

87 investigate changes of cathodically protected systems in time. Specimen without a holiday were

88 treated as a reference samples. Differences between samples without coating disruptions and

89 intentionally defected samples and their time evolution under four CP protection levels regimes were

90 anticipated to be observed.

91 Defect free specimen without CP during the experiment exhibited a straight-like line in their Bode

92 spectrum (Fig. 2). Phase angle was very close to 90° in the entire frequency range. A slight shift towards

93 lower phase angles was observed in the low frequency range only, approaching a DC limit. A capacitive

94 nature of the response suggests that the coating remains intact during entire exposure. Positive phase

95 angle shift at the lowest frequencies indicates slow coating deterioration. Its character became more

96 resistive. Impedance modulus at low frequencies remained higher than 10^9 Ω. If a surface area of the

97 specimen is taken into account it translates to approximately $2,8 \cdot 10^{10}$ Ωcm^2. The impedance modulus

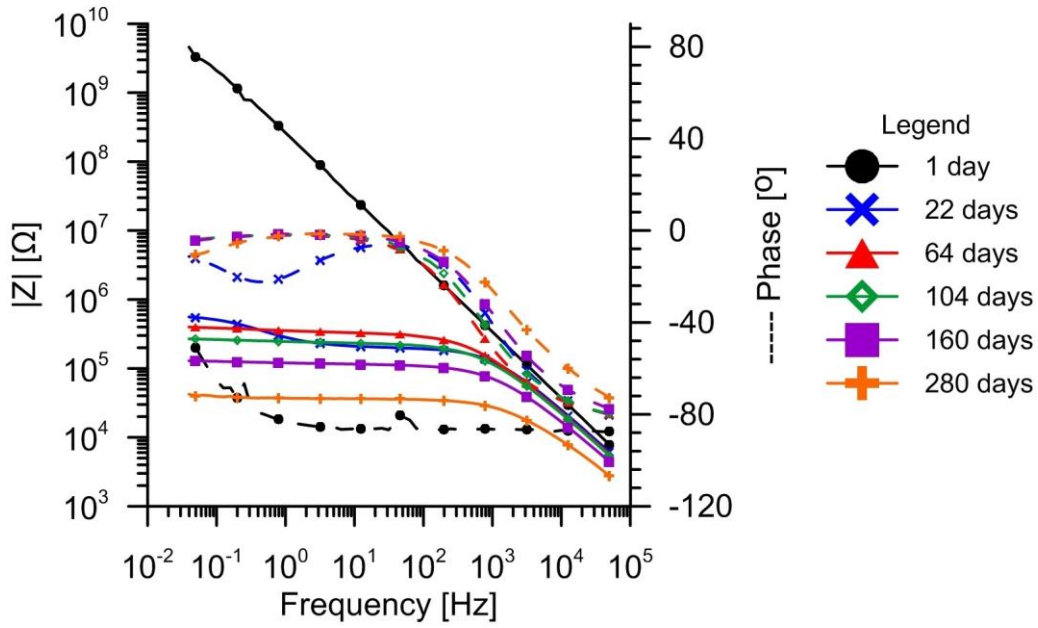98 and phase angle measured were characteristic for an unbroken, intact and fully protective coating (2).

99 Unlike in the case of the unprotected sample, the other specimen show indications of coating

100 deterioration. It is more than likely that the cathodic protection accelerates coating deterioration.

101 Characteristic spectra evolution of the fully coated specimen were observed for all samples with any

102 degree of cathodic protection (Fig. 3-5). In the first spectrum taken (at the beginning of the

103 experiment) impedance modulus forms an almost straight line. Phase shift was lower than -40^0 even

104 at the lowest frequencies. The coating had a capacitive character. During the exposure an impedance

105 modulus plateau had formed. Once the plateau was observed a distinctive phase shift became visible.

106 Impedance of the system had a 0° phase angle at the lowest frequencies and -90° at higher frequencies.

107 It indicated that coating nature had changed from purely capacitive (an intact coating) to resistive.

108 When time passed the phase shift from 0° to 90° started occurring at higher and higher frequencies.

109 The impedance modulus plateau value decreased. Plateau bandwidth was greater too, as the phase

110 shift 'moved' towards higher frequencies. After the exposure the CP protected samples still exhibited

111 some degree of protection.

112 Equivalent circuits with either one or two time constants fitted measured EIS spectra. Values of chi

113 squared (X^2) which is a measure describing discrepancies between measured values and a model under

114 investigation are presented for every figure which involves EIS model fitting. A model with two time

115 constants was chosen for spectra which showed an indication of a second semicircle formation.

116 Evolution of coating resistance is presented in Fig. 6. After quick initial breakdown all of the coatings

117 reached a resistance plateau. Calculated coating capacity is presented in Fig. 7. Initial capacity and

118 resistance of all coatings is almost the same – they have been applied in the same manner and had a

119 similar thickness. All of them quickly increased their capacity due to water uptake. Then coating

120 capacity did not increase any further and it remained stable for the entire duration of the experiment.

121 The under protected sample exhibited impedance lower than 10^6 Ωcm^2 – a border line value for a
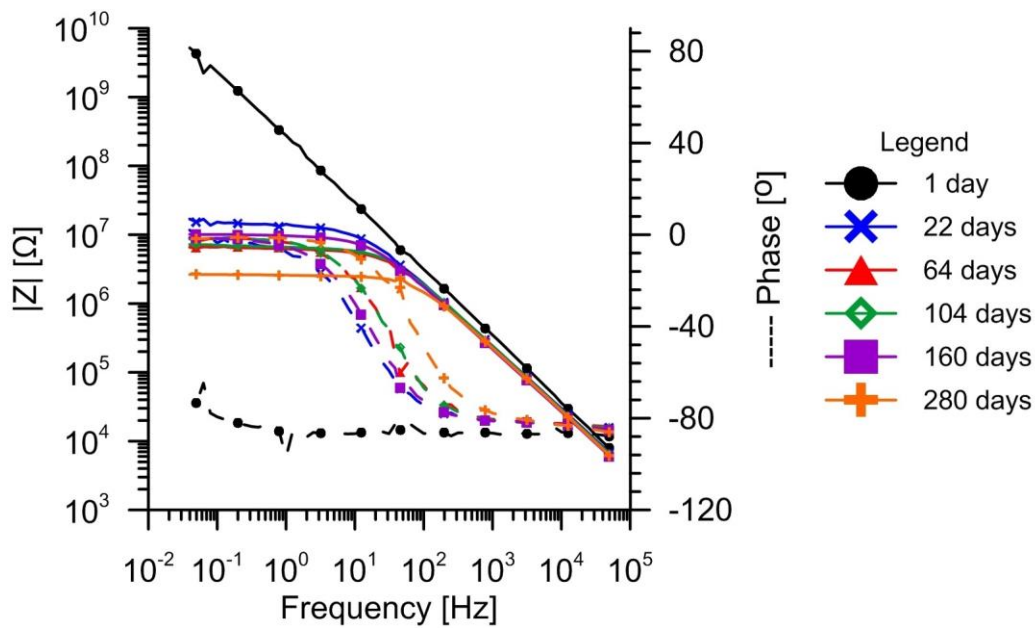
122 protective coating.

123

124 Fig. 2 Exemplary EIS Bode plots of CP unprotected defect-free organic coated specimen in time. To

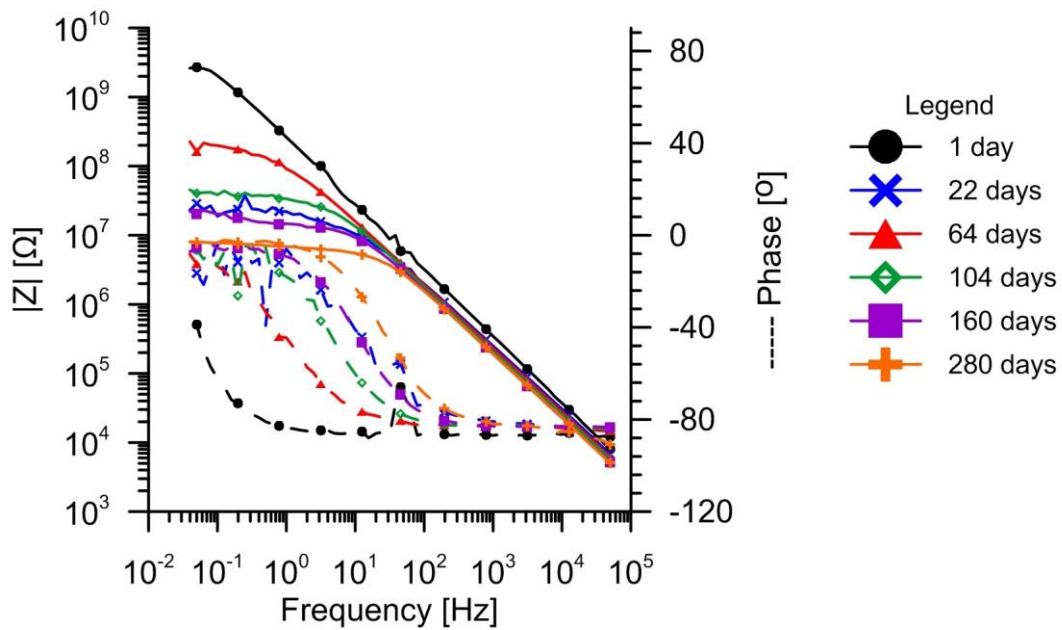125 clarify the chart not every obtained plot is presented.

Fig. 3 Exemplary EIS Bode plots of CP under protected defect-free organic coated specimen in time. To clarify the chart not every obtained plot is presented.
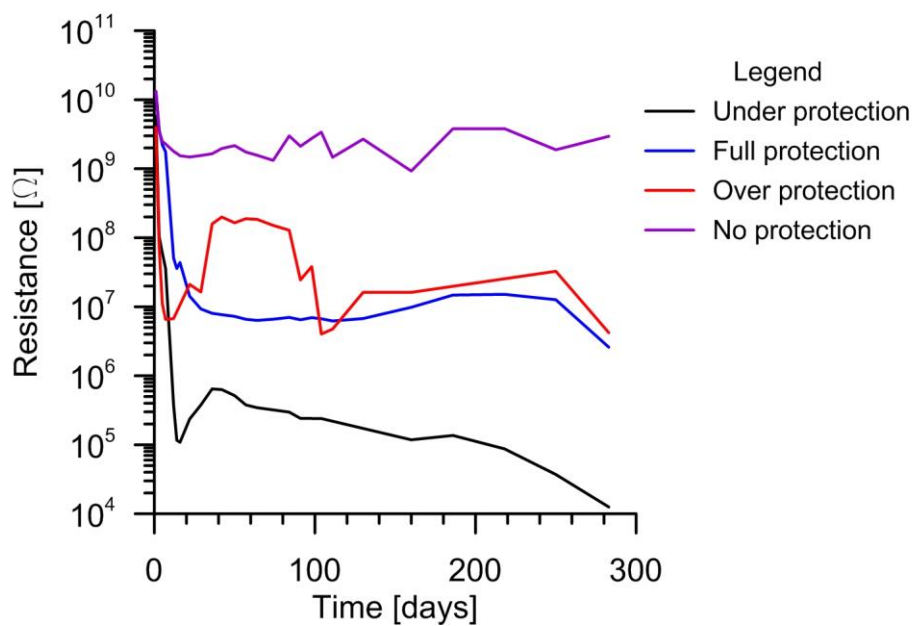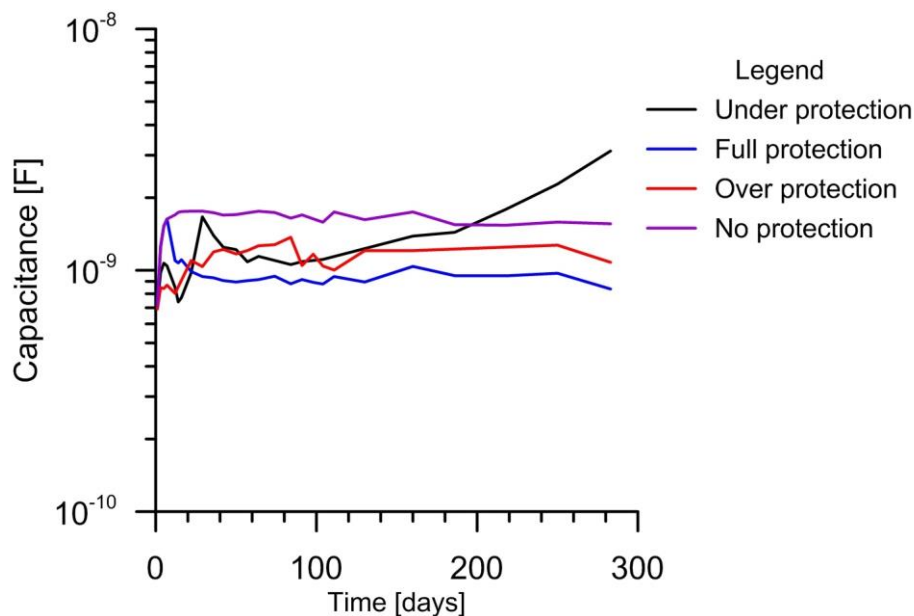

Fig. 4 Exemplary EIS Bode plots of CP fully-protected defect-free organic coated specimen in time. To clarify the chart not every obtained plot is presented.

132

133   Fig. 5 Exemplary EIS Bode plots of CP overprotected defect-free organic coated specimen in time. To

134   clarify the chart not every obtained plot is presented.

135

136   Fig. 6 Coating resistance vs time plot based on equivalent circuit model fit to the measured EIS spectra.

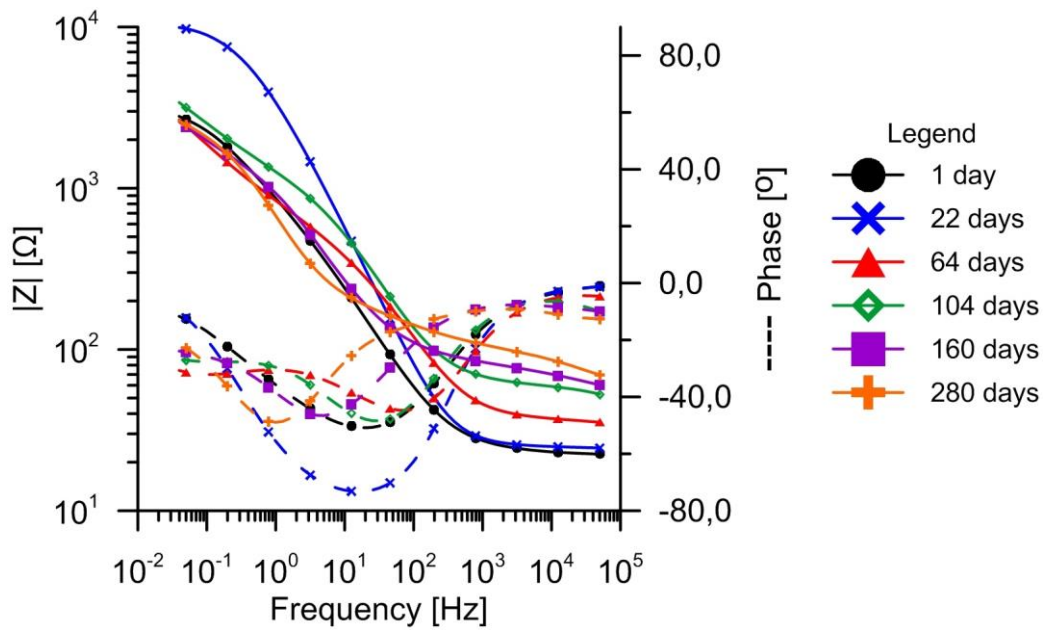137   Chi squared (X2) – goodness of fit values ranged from $3,45 \cdot 10^{-4}$ to $1,04 \cdot 10^{-2}$.

138

139 Fig. 7 Coating capacity vs time plot based on equivalent circuit model fit to the measured EIS spectra.

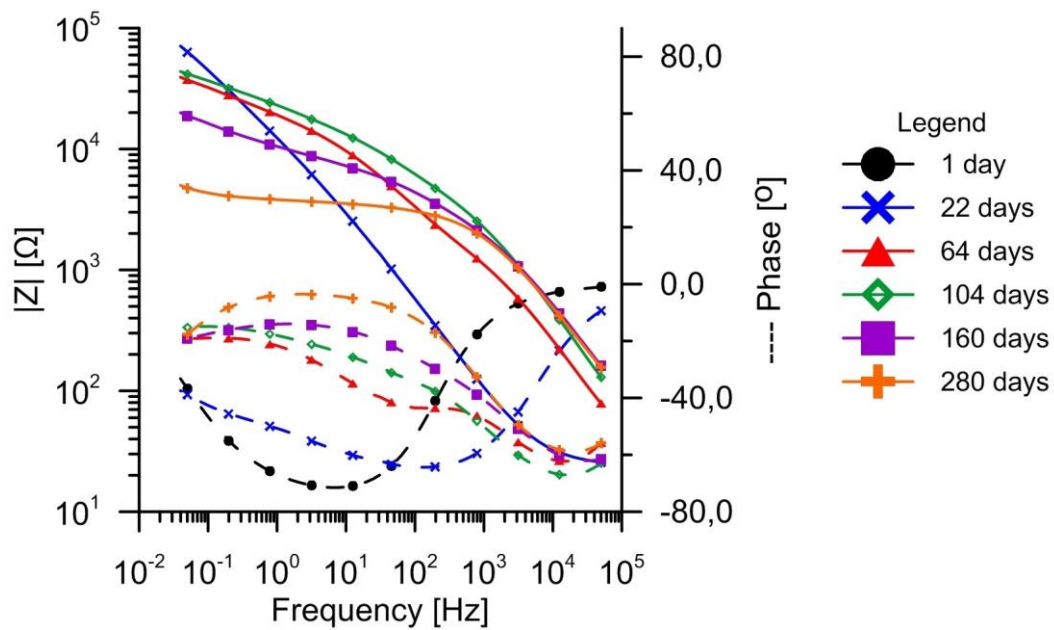140 Chi squared (X2) – goodness of fit values ranged from $3{,}45 \cdot 10^{-4}$ to $1{,}04 \cdot 10^{-2}$.

141 Spectra of an unprotected organic coated sample with a ϕ0,5 cm holiday are presented in Fig. 8. All of

142 the spectra resemble a one time-constant system. A distinctive phase angle peak is visible, initially at

143 approximately $2 \cdot 10^{1}$ Hz. The peak is shifted in time towards lower frequencies down to 1 Hz. However,

144 it must be noted that there are two reactions occurring simultaneously – iron oxidation and oxygen

145 reduction which cannot be distinguished with EIS.

146 Spectra of an under protected and fully protected organic coated sample with a ϕ0,5 cm holiday are

147 presented in Fig. 9 and Fig. 10. Both of these cases are described together because their similarities

148 can be immediately noticed. Initially, on a 1st day of exposure a phase peak is visible at frequency of

149 10 Hz (Fig. 9) and 100 Hz (Fig. 10). As time passed their phase angle flattened. At low and medium

150 frequency bandwidth the response of the system became resistive (0° phase angle) and at higher

151 frequencies it changed became more capacitive. Impedance modulus plateau appeared when phase

152 angle approached zero at low and medium frequencies. It could be attributed to coating deterioration.

153 Rising alkalinity of the environment due to oxygen reduction and increase of OH^{-} content might be the

154 cause of this phenomenon. Accurate model fit to those EIS cases is troublesome due to the overlapping

155 time constants. Flat and elongated Nyquist spectra for under protected and fully protected specimen
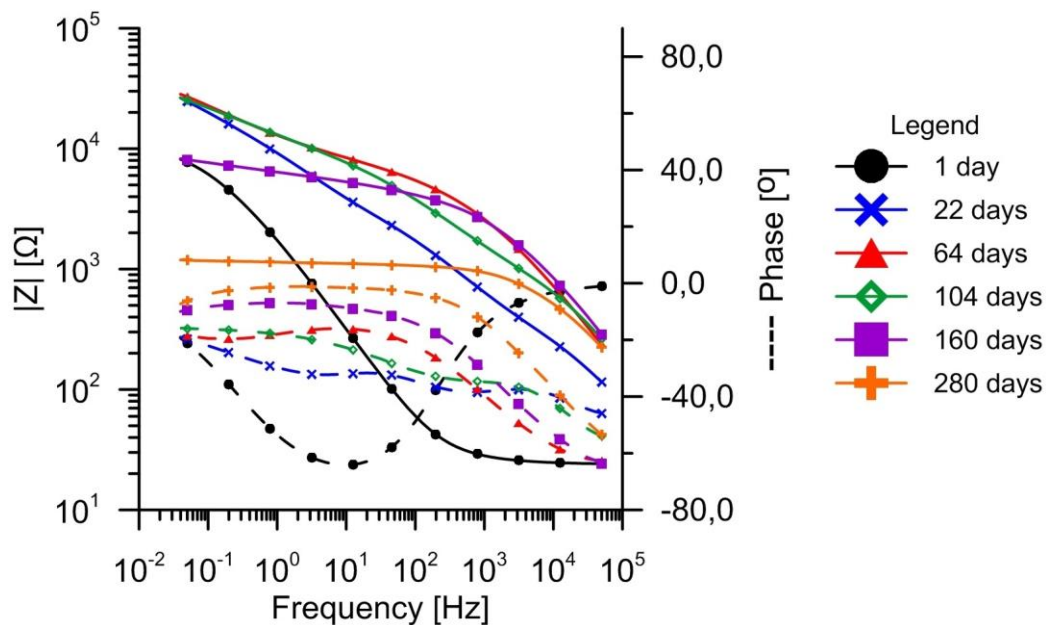
156 are presented in Fig. 11.

157

158 Fig. 8 Exemplary EIS Bode plots of CP unprotected organic coated specimen with a φ0,5 cm defect, in

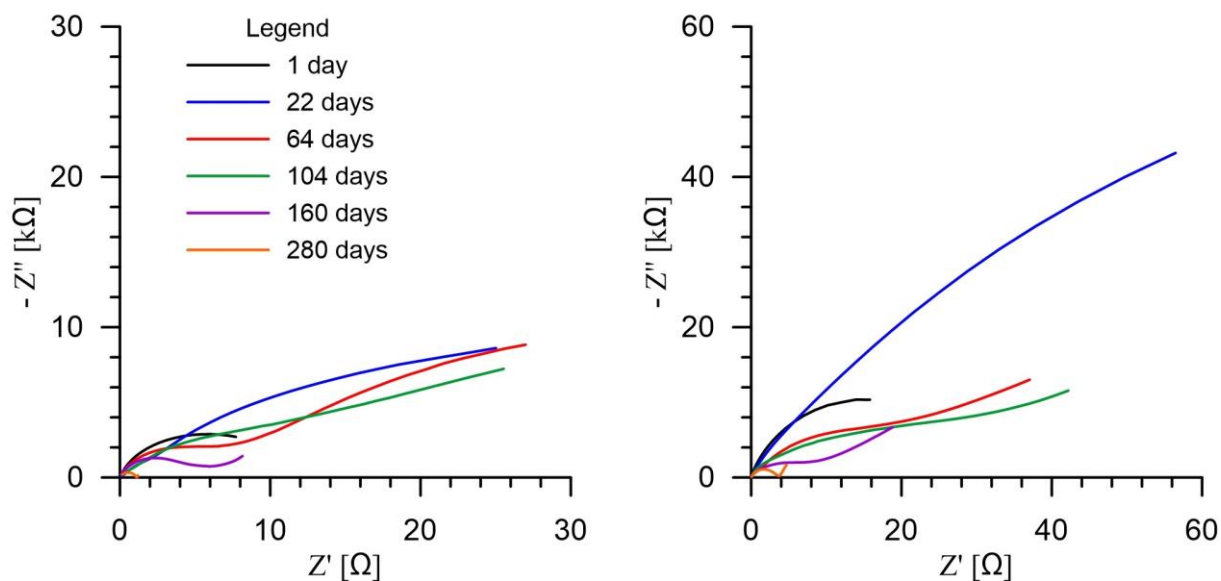159 time. To clarify the chart not every obtained plot is presented.

160

161 Fig. 9 Exemplary EIS Bode plots of CP under protected organic coated specimen with a φ0,5 cm defect,

162 in time. To clarify the chart not every obtained plot is presented.

163

Fig. 10 Exemplary EIS Bode plots of CP fully protected organic coated specimen with a φ0,5 cm defect, in time. To clarify the chart not every obtained plot is presented.
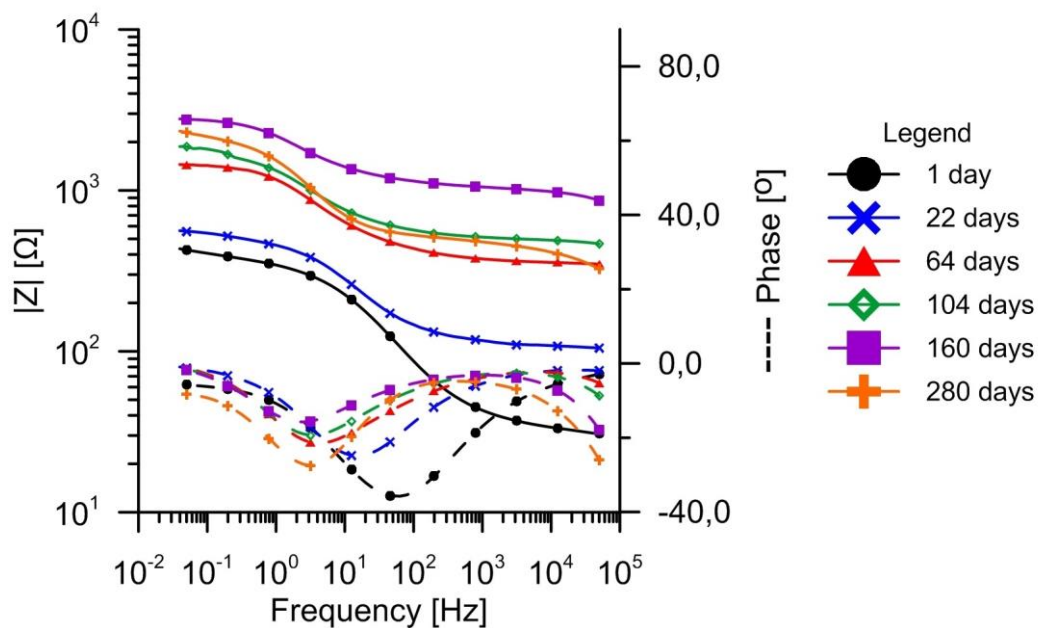

166

Fig. 11 Exemplary EIS Nyquist plots of CP under protected (left) and fully protected (right) organic coated specimen with a φ0,5 cm defect, in time. To clarify the chart no every obtained plot is presented.
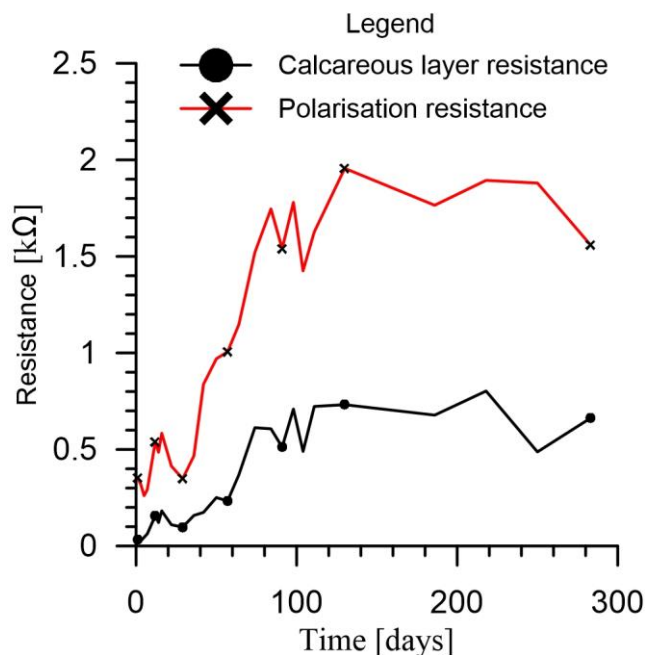
Bode phase spectra of overprotected sample with a coating have a distinct peak (Fig. 12). Initially the peak appeared at approximately 10^2 Hz. Naturally overprotection (sample's potential of -1200 mV vs Ag|AgCl|seawater) involves occurrence of a fast reaction – water decomposition. In time the phase angle peak shifted towards lower frequencies, up to approximately 1 Hz. This phenomena could be

174 linked to the calcareous sediment layer evolution. Expanding calcareous layer reduces the active

175 surface and the reaction eventually slows down. The phase peak is shifted towards lower frequencies.

176 Unlike other specimen the impedance modulus spectra is shifted up in time. A new high frequency

177 phase shift became more distinct later on. In a Nyquist plot it is visible as part of a second semicircle

178 (Fig. 12). Its appearance can be most likely linked to the calcareous layer. It proves that the sediments

179 reduce the reaction rate as the overall impedance modulus is increased. In case of the unprotected

180 sample there is no distinct shift of the impedance modulus (with an expectation of the initial increase

181 due to corrosion products formation). It can be assumed that the system response in the investigated

182 frequency range is associated with water decomposition reaction and evolution of calcareous layer. In

183 order to determine the evolution of polarisation resistance and calcareous layer resistance equivalent

184 circuit model was fitted to the experimental data. Those quantities are presented in Fig. 13. The fact

185 that sediment layer resistance increased in time proved its development and reduction of reactive

186 surface area. As a result rate of water decomposition reaction declined and fitted polarisation

187 resistance increased.

189 Fig. 12 Exemplary EIS Bode plots of CP overprotected organic coated specimen with a ϕ0,5 cm defect,

190 in time. To clarify the chart not every obtained plot is presented.

Fig. 13. Plot of polarisation resistance and calcareous layer resistance in time based on equivalent circuit model fit to the measured EIS spectra. Overprotected ϕ0,5 cm defected coating specimen. Chi squared (X2) – goodness of fit values ranged from $2,13 \cdot 10^{-5}$ to $7,45 \cdot 10^{-3}$.

Corrosion rates determined from weight loss coupons for unprotected, under protected, fully protected and overprotected were as follows: 0,073 mm/year, 0,007 mm/year, 0,003 mm/year, 0,002 mm/year. Obtained corrosion rates and their relative relations are reasonable and in accordance with values reported in literature for corresponding cathodic protection degrees.

4. Conclusions

Long term exposures of defect-free and ϕ0,5 cm defected epoxy coated specimen in four different cathodic protection conditions in artificial seawater were performed. Exposures lasted for over 9 months. Time evolution of spectra of investigated coatings was recorded.

An evolution of EIS spectra of a defect-free sample in all four CP conditions was similar and was characteristic for a deteriorating coating. However the coating deterioration with any degree of cathodic protection underwent quicker than in conditions without cathodic polarization. A CP unprotected coating retained its protective properties for the entire experiment without any major signs of a coating failure. Protective organic coating condition could be estimated and monitored in time based on EIS investigations.

209 Both overprotected and unprotected samples with a φ0,5 cm defect had a characteristic impedance
210 spectra in the investigated frequency range. Their time evolution was described. If a sample is defected
211 EIS allows a recognition of overprotected and unprotected sample.

212 Under protected and fully protected samples have similar spectra. Their evolution in time is also akin,
213 same features are observed in their spectra and they evolve in the same pattern. However, the spectra
214 evolution of a fully protected sample is significantly quicker. Distinguishing a fully protected sample
215 from under protected sample based on EIS only is troublesome.

216 EIS is capable of providing additional information complementary to ordinary current and potential
217 measurements. Based on the laboratory experiments a test electrode could be applicable as an
218 additional information source of coating's sample condition. However the EIS data is troublesome to
219 be analysed in situ. Data could be easily transferred from multiple measurement units and
220 stored/transferred for analysis.

221 5. Acknowledgements

224 6. References

225 1. Z. W. Wicks Jr., F. N. Jones, S. P. Pappas, D. A. Wicks. Organic Coatings: Science and Technology. s.l.
226 John Wiley & Sons, 2007.

227 2. P. A. Sørensen, S. Kiil , K. Dam-Johansen, C. E. Weinell, Anticorrosive coatings: a review, J. Coat.
228 Technol. Res. 6 (2009) 135-176.

229 3. M. Zubielewicz, W. Gnot, Mechanisms of non-toxic anticorrosive pigments in organic waterborne
230 coatings, Prog. Org. Coat. 49 (2004) 359-371.

231 4. G. Williams, H.N. McMurray, M. J. Loveridge, Inhibition of corrosion-driven organic coating
232 disbondment on galvanised steel by smart release group II and Zn(II)-exchanged bentonite pigments,
233 Electrochim. Acta. 55 (2010) 1740-1748.

234 5. V. Ashworth, C.J.L. Booker. Cathodic protection: Theory and practice, John Wiley and Sons, New
235 York, 1986.

236 6. Seong-Jong Kim, Masazumi Okido, Kyung-Man Moon, An electrochemical study of cathodic
237 protection of steel used for marine structures, Korean J. Chem. Eng. 20 (2003) 560-565.

7. F. Gan, Z. W. Sun, G. Sabde, D. T. Chin, Cathodic Protection to Mitigate External Corrosion of Underground Steel Pipe Beneath Disbonded Coating, Corros. Eng. 50 (1994) 804-816.

8. K. Zakowski, Studying the effectiveness of a modernized cathodic protection system for an offshore platform, Anti-Corros. Method. M. 58 (2011) 167-172.

9. L. Martinez, L. V. Žulj, F. Kapor, Disbonding of underwater-cured epoxy coating caused by cathodic protection current, Corr. Sci. 51 (2009) 2253-2258.

10. Y. R. Yoo, H. H. Cho, S. Take, J. G. Kim, Y. S. Kim, Influence of cathodic protection on the lifetime extension of painted steel structures, Met. Mater. Int. 12 (2006) 255-261.

11. E. L. Koehler, The Mechanism of Cathodic Disbondment of Protective Organic Coatings—Aqueous Displacement at Elevated pH, Corr. Sci. 40 (1984) 5-8.

12. T. Kamimura, H. Kishikawa, Mechanism of Cathodic Disbonding of Three-Layer Polyethylene-Coated Steel Pipe, Corr. Sci. 54 (1998) 979-987.

13. C.F. Barth, A. R. Troiano, Cathodic Protection and Hydrogen in Stress Corrosion Cracking, Corrosion 28 (1972) 259-263.

14. L.H. Wolfe, C.C. Burnette, M.W. Joosten, Hydrogen embrittlement of cathodically protected subsea bolting alloys, Mater. Performance 32 (1993).

15. D, Festy, Cathodic Protection of Steel in Deep Sea: Hydrogen Embrittlement Risk and Cathodic Protection Criteria, Corrosion 2001, Conference materials.

16. R. W. Bosch, J. Hubrecht, W. F. Bogaerts, B. C. Syrett, Electrochemical Frequency Modulation: A New Electrochemical Technique for Online Corrosion Monitoring, Corr. Sci. 57(2001) 60-70.

17. C. Andrade, C. Alonso, Corrosion rate monitoring in the laboratory and on-site, Constr. Build. Mater. 10 (1996) 315-328.

18. J. P. Broomfielda, K. Davies, K. Hladky, The use of permanent corrosion monitoring in new and existing reinforced concrete structures, Cement Concrete Comp. 24 (2002) 27-34.

19. K. Zakowski, W. Sokolski, 24-hour characteristic of interaction on pipelines of stray currents leaking from tram tractions, Corr. Sci. 41 (1999) 2099-2111.

20. K. Żakowski, K. Darowicki, Methods of Evaluation of the Corrosion Hazard Caused by Stray Currents to Metal Structures Containing Aggressive Media, Pol. J. Environ. Stud. 9 (2000) 237-241.

21. K. Zakowski, K. Darowicki, Diagnosis of Reference Electrodes in Cathodic Protection Systems by Electrochemical Impedance Spectroscopy, Corros. Rev. 20 (2011) 391-402.

268   22. Guofu Qiao, Jinping Oua, Corrosion monitoring of reinforcing steel in cement mortar by EIS and

269   ENA, Electrochim Acta 52 (2007) 8008-819.

270   23. M. Szocinski, K. Darowicki, Local impedance spectra of organic coatings, Polym. Degrad. Stabil. 98

271   (2013) 261-265.

272   24. S. Krakowiak, K. Darowicki, Inspection of rubber linings operating in flue gas desulphurisation units,

273   Prog. Org. Coat. 46 (2003) 211-215.

274   25. K. Darowicki, P. Slepski, M. Szocinski, Application of the dynamic EIS to investigation of transport

275   within organic coatings, Prog. Org. Coat. 52 (2005) 306-310.

276   26. NACE International, NACE No. 2/SSPC-SP 10 White Metal Blast Cleaning.

277   27. ASTM International. ASTM D1141 - 98 Standard Practice for the Preparation of Substitute Ocean

278   Water, 2013.